Ultrasound Induces Aging in Granular Materials

David Espíndola, Belfor Galaz, and Francisco Melo

Departamento de Física, Universidad de Santiago de Chile, Avenida Ecuador 3493, Casilla 307, Correo 2, Santiago, Chile

(Received 26 July 2012; published 9 October 2012)

Aging and rejuvenation have been identified as the general mechanisms that rule the time evolution of granular materials subjected to some external confinement pressure. In *creep* experiments performed in a triaxial configuration, we obtained evidence that relatively high intensity ultrasound waves propagating through the material induce both weakening and significant plasticity. In the framework of *glassy materials*, it is shown that the effect of ultrasound can be simply accounted for by a general variable, the *fluidity*, whose dynamics are described by an effective aging parameter that strongly decreases with sound amplitude and vanishes at the yield stress limit. The response from step perturbations in ultrasound intensity provided a method to assess the effective-viscosity jumps which are direct evidence of acoustic fluidization.

DOI: 10.1103/PhysRevLett.109.158301 PACS numbers: 83.80.Fg, 62.20.Hg, 83.60.La

Despite the apparent *athermal* character of granular packing, experimental evidence has grown to show a slow aging of such materials when maintained at a constant stress, below the yield stress. For instance, tiny vibrations [1] or thermal cycling [2] have been shown to drive important packing reorganization attributed to surface roughness and contact plasticity, which both take place at a sub-granular scale. Recently, Nguyen and co-workers [3] have applied a *glassy materials approach*, in which a parameter named fluidity is employed to account for the rate of strain relaxation of a granular packing. A logarithmic strain relaxation was evidenced and the resulting creep dynamics were rescaled onto a unique curve characterized by an effective aging parameter.

On the other hand, sound velocity measurements reveal softening of granular compact at large wave amplitudes due to frictional nonlinearities at the grain's contacts, but contact reorganization and sliding are not necessarily involved [4]. This softening has been observed both by direct measurements of wave propagation and by the investigation of the frequency shifts in resonance experiments performed in oedometer cells [5]. High amplitude acoustic waves, even near the jammed granular state, may indeed induce local contact sliding along with significant decrease in material viscosity. Enlightening information on the structural changes of the material has been obtained recently by Jia *et al.* by using sound diffusion (coda wave) in both oedometric [4,6] and shear cells [7]. This effect, described first by Melosh [8,9], is called *acoustic fluidization* and has been applied to explain the weakening of faults in a geophysical context. The small failure events of stick slip induced by acoustic waves in granular media and its connection with earthquake triggering is another manifestation of the same phenomenon [10]. However, to our knowledge, only indirect evidence of acoustic fluidization has been achieved due to difficulties found in the assessment of the rheological properties of granular materials [11]. In this Letter, we examine the effect of high amplitude ultrasonic waves on the time relaxation of a material at constant external stress in the *triaxial configuration*: a creep test. Our system allows us to independently control longitudinal as well as transverse stress and thus to approach the yield stress limit from below. First, we show that in the absence of ultrasound, the slow relaxation of granular compact shares similar features as that described recently in Ref. [3] and that an effective aging parameter, which vanishes at the yield stress, can be defined, regardless of differences in experimental configuration. In the presence of ultrasound, the aging parameter is found to decrease strongly with wave amplitude. We use correlations of diffusive waves [12] to identify irreversible particle-contact rearrangements during the creep process. The strain rate's response to a step in the ultrasonic amplitude indicates that the effective viscosity jumps to lower values with step amplitude. Viscosity variations are only qualitatively captured by early predictions of acoustic fluidization. We propose a simple generalization of Melosh's model to quantitatively account for our findings.

The granular sample consists of dry polydisperse glass beads of diameter $d = 0.9$–1.2 mm confined by a cylindrical latex membrane, which is closed hermetically at its extremes by two ultrasound transducers, Fig. 1. The sample is prepared by pouring a fixed mass ($M = 37g$) of granular material into the latex container whose shape is fixed by a dural-aluminium cylindrical mold, of height $h = 20$ mm and diameter $D = 40$ mm, which produces a packing fraction of $\phi \approx 0.63$. Before removing the mold, the interstitial air is evacuated by means of a vacuum pump ensuring a constant confinement pressure, $P_0 \approx 93$ kPa. The sample is then mounted in the creep test system where a constant uniaxial load σ_{ext} ranging from 15 to 80 kPa is applied. An inductive position sensor records the axial deformation. Thus, the strain-relaxation behavior is followed while sound speed and *speckle correlation* are

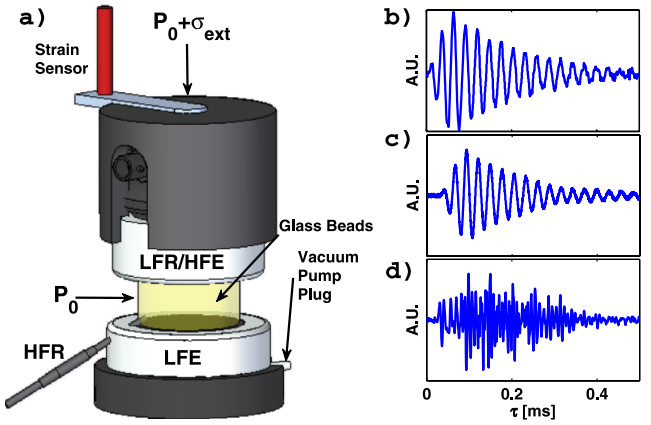

FIG. 1 (color online). (a) Experimental setup. Top transducer is either a high frequency emitter (HFE) or low frequency receptor (LFR). LFE is the low frequency emitter and HFR indicates the high frequency miniature receptor. (b) Acoustic signal in LFE measured directly by a laser vibrometer. (c) Typical coherent wave received by LFR. (d) Typical coda wave received by HFR.

monitored by suitable ultrasonic transducers. Placed at the bottom, a low frequency emitter (LFE) transducer of active area 42 mm is used to provide a coherent train wave of 2 cycles at 40 kHz ($\lambda \approx 16d$), every 1 s. The vibration amplitude ϵ_{US} of this transducer was calibrated directly, in terms of displacement, by means of a laser Doppler vibrometer (Polytec Inc., Germany). Depending on the variable monitored during the creep test, at the top part of the cell we place either a low frequency receptor transducer (LFR, identical to LFE) to detect the coherent wave and measure its sound speed, or a high frequency emitter transducer (HFE, 30 mm of diameter) to transmit a 2 cycle train wave of 320 kHz ($\lambda \approx 2d$) every 200 ms to excite acoustic speckles. The latter propagate diffusively through the sample and are captured by a high frequency miniature transducer (HFR).

First, we perform experiments to capture the relaxation features at different uniaxial loads. Indeed, a logarithmic time dependence is observed for the strain [Fig. 2(a)]. As discussed in Ref. [3] and inspired by the work of Derec *et al.* [13], a fluidity parameter $f = G/\eta$, which represents a time dependent rate for stress relaxation, can be introduced to quantitatively analyze such behavior. Here G and η are the elastic modulus and an effective viscosity of the bulk, respectively. In the context of complex fluid rheology, the dynamics of f are given by the simplest and lowest order coupling involving natural aging and stress rejuvenation. This is,

$$\dot{\sigma} = -f\sigma + G\dot{\gamma} \qquad \dot{f} = -af^2 + r\dot{\gamma}^2, \tag{1}$$

where γ is the strain and a and r are the parameters controlling aging (f decrease) and rejuvenation (f increase), respectively, and σ is the deviatoric stress. In our configuration, the deviatoric stress is simply σ_{ext},

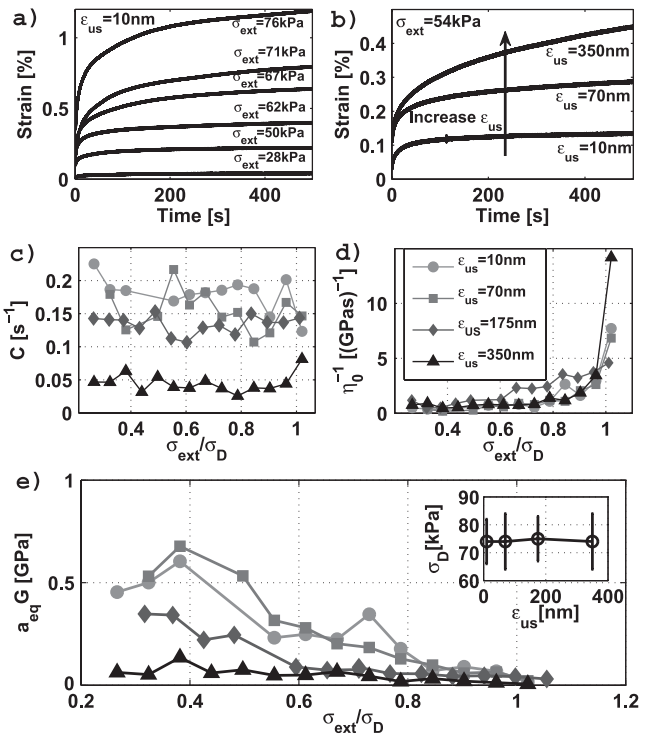

FIG. 2. (a) Creep curves for constant $\epsilon_{\mathrm{US}} = 10$ nm and increasing σ_{ext} from 20 to 80 kPa. (b) Creep curves at constant $\sigma_{\mathrm{ext}} = 54$ kPa and distinct ϵ_{US}. (c) Parameter $C = a_{\mathrm{eq}}f_0$ obtained by fitting experimental data with Eq. (3). (d) Inverse of initial viscosity, $1/\eta_0 = f_0/G$ obtained from the initial slope of the creep curves shown in (a) and (b). (e) Time rate of the effective viscosity $a_{\mathrm{eq}}G = C\eta_0$ against σ_{ext} for distinct ϵ_{US}. Inset: The experimental value of σ_D (σ_{ext} for which $a_{\mathrm{eq}}G$ vanishes) is independent of ϵ_{US}. In (c)–(e) σ_{ext} is normalized to $\sigma_D \approx 75$ kPa.

which is kept constant in creep experiments, leading to $f = \frac{G\dot{\gamma}}{\sigma_{\mathrm{ext}}}$. Thus,

$$\dot{f} = -a_{\mathrm{eq}}f^2, \tag{2}$$

where $a_{\mathrm{eq}} = a(1 - \frac{\sigma_{\mathrm{ext}}^2}{\sigma_D^2})$ is the effective aging parameter defined in Ref. [3] and $\sigma_D \equiv \sqrt{a/r}G$ is the stress for which a_{eq} vanishes. Solving Eq. (2) leads to

$$\gamma(t) = \frac{\sigma_{\mathrm{ext}}}{Ga_{\mathrm{eq}}} \log(1 + a_{\mathrm{eq}}f_0 t). \tag{3}$$

Writing $\gamma(t) = \frac{\sigma_{\mathrm{ext}}f_0}{GC} \log(1 + Ct)$ with $C = a_{\mathrm{eq}}f_0$, where f_0/G can be found by using $f_0/G = \dot{\gamma}_0/\sigma_{\mathrm{ext}}$ from the initial slope of strain time evolution, the constant C is the only adjustable parameter to fit the experimental data. In Fig. 2(a), fits are indistinguishable from the experimental points. The corresponding values of C and f_0/G as a function of σ_{ext} are presented in Figs. 2(c) and 2(d), respectively. Since the effective viscosity obeys $\eta(t) = a_{\mathrm{eq}}Gt + G/f_0$ and G is nearly constant during creep experiments, $a_{\mathrm{eq}}G$ and G/f_0 can be interpreted as the viscosity rate and the initial viscosity η_0, respectively.

As shown in Fig. 2(c), C is nearly independent of σ_{ext}, while η_0^{-1} exhibits a significant increase for $\sigma_{\text{ext}} \rightarrow \sigma_D$; Fig. 2(d). In turn, the time rate $a_{\text{eq}}G$ decreases with σ_{ext} and vanishes for $\sigma_{\text{ext}} = \sigma_D \approx 75$ kPa; Fig. 2(e).

The creep experiments are then repeated for distinct ϵ_{US}, ranging from 10 to 350 nm; Fig. 2(b). Interestingly, the presence of ultrasound induces a gradual but significant enhancement to the relaxation process, which can be characterized by the parameters extracted from the logarithmic fit. Indeed, in the presence of ultrasound, the parameter C is practically independent of the applied external load, but decreases with the ultrasound amplitude; Fig. 2(c). For all values of ϵ_{US} explored, η_0^{-1} increases rapidly with σ_{ext} when σ_{ext} approaches σ_D; Fig. 2(d). However, the effect of increasing ϵ_{US} on η_0^{-1} is not clearly revealed. In turn, $a_{\text{eq}}G$ decreases with both ϵ_{US} and σ_{ext} vanishing for $\sigma_{\text{ext}} \approx 75$ kPa regardless of the ultrasound intensity. Thus, σ_D is constant for a given confining pressure P_0; inset Fig. 2(e).

To better characterize the effect of ultrasound on G and η we explore the effect of a sudden increase of ultrasonic intensity on the creep process (step response). The creep is first followed for $\epsilon_{\text{US}} = 10$ nm and at a time, t_s, the ultrasound jumps to a higher amplitude ϵ_{US}. Subindex "$-$" and "$+$" indicate the variables just before and immediately after the step in ϵ_{US} is introduced, respectively. The strain is continuous, whereas, an abrupt change in the strain rate is observed at t_s, Figs. 3(a) and 3(b). Such a discontinuity in strain rate increases with the step amplitude ϵ_{US} and decreases with σ_{ext}. Panels (c) and (d) in Fig. 3 indicate that sound speed c is a function of the ultrasound step but it is nearly independent on σ_{ext}. Indeed, the system weakens with increasing ϵ_{US}. Weakening has been reported recently by Jia *et al.* [4] and previously in resonance experiments by Johnson and Jia [5]. Despite differences in cell geometry, from the shift in the resonance frequency as a function of ϵ_{US}, we obtained identical weakening (data not shown) as that reported in Ref. [5]. To obtain insight about structural modification during creep, the contact force network was monitored by using the global correlation of two consecutive multiple scattered waves. The high sensitivity of this wave to tiny irreversible modifications in the contact network has been demonstrated recently in Ref. [4]. The maximum value of this correlation, $\rho_i \rho_{i-1}$, is computed in the usual way [4], and its temporal evolution is shown in Figs. 3(e) and 3(f). An abrupt loss of correlation is observed when the ultrasonic perturbation is suddenly increased. The correlation then recovers in time, revealing a competition between the aging and the ultrasound-induced rejuvenation. Roughly, the degree of decorrelation is proportional to the jump in ultrasound amplitude and practically independent of σ_{ext}.

The weakening effect due to ϵ_{US} steps is summarized in Fig. 4(a). The absolute value of $\Delta c/c_-$ increases with ϵ_{US} and this tendency is practically independent of σ_{ext}, which can also be visualized from Fig. 3(d). In Ref. [4], a linear dependence of $\Delta c/c_-$ with ϵ_{US} was observed and attributed to the hysteretic behavior of the contact force between grains during a cycle. Our data are compatible with this behavior at low ϵ_{US}. However, since we explored a wider range of ϵ_{US}, $\Delta c/c_-$ reveals an additional feature: it tends to saturate at high levels of ϵ_{US}. We believe that this saturation occurs when the irreversible structural changes, taking place at the contact level, and dominates over the number of reversible contacts. Qualitatively, this saturation is consistent with a decrease in the coda correlation, at similar levels of ϵ_{US}. In the framework of the fluidity function, the strain rate response to steps on ϵ_{US} can be accounted for by considering instantaneous adjustment in both the effective viscosity

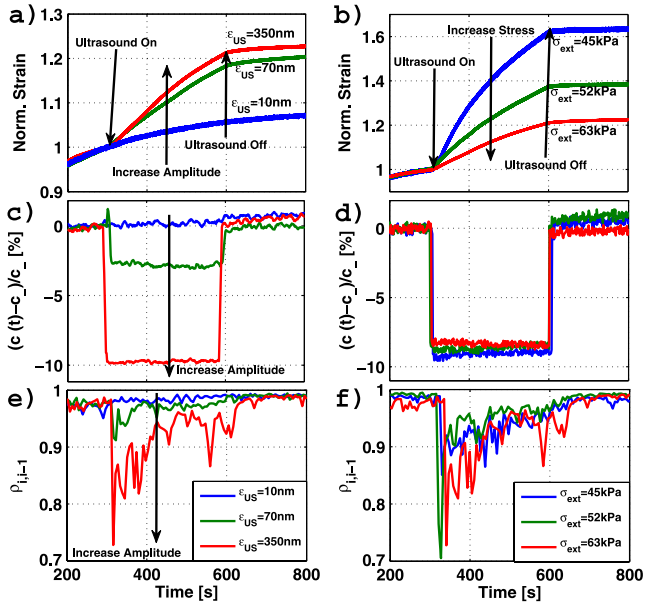

FIG. 3 (color online). (a) Sample strain for increasing steps in ϵ_{US} at constant $\sigma_{\text{ext}} = 45$ kPa. (b) Sample strain for constant step $\epsilon_{\text{US}} = 350$ nm and distinct σ_{ext}. (c) and (d) Sound speed variations, in response to the ultrasonic steps used in (a) and (b), respectively. (e) and (f) Maximum global correlation of consecutive coda waves for similar condition than (a) and (b), respectively.

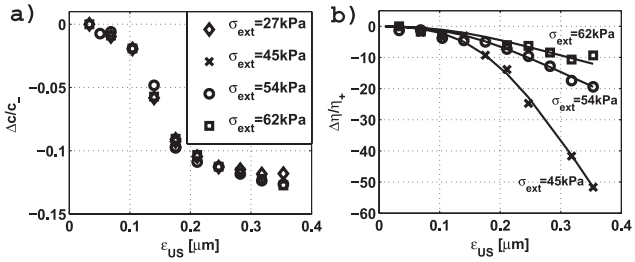

FIG. 4. (a) Relative sound speed jumps observed in Fig. 3(c) vs ϵ_{US}. (b) Relative jumps in effective viscosity from strain rate discontinuity, in $t = t_s$, given by Eq. (4), as a function of ϵ_{US}. Solid lines are the best fits from the Eq. (6) with $\alpha = 5.8 \times 10^3$ and $\beta = 0.18$.

and the elastic modulus. Given that $f = \frac{G}{\eta} = \frac{G}{\sigma_{\rm ext}}\dot{\gamma}$, this leads to

$$\frac{\Delta\dot{\gamma}}{\dot{\gamma}_-} = -\frac{\Delta\eta}{\eta_+}. \quad (4)$$

This equation is then used to relate the abrupt increment of the strain rate shown in Figs. 3(a) and 3(b) with the sudden increase of the effective viscosity. The relative viscosity changes, $\frac{\Delta\eta}{\eta_+}$, illustrated in Fig. 4(b), indicate that the effective viscosity decreases with increasing $\epsilon_{\rm US}$. Interestingly, the effect of ultrasound amplitude on the effective viscosity is more pronounced at lower values of $\sigma_{\rm ext}$.

To account for our experimental finding, let us consider each particle like a slider of friction coefficient μ, subjected to both a shear stress τ and a normal stress P_c, whose average values relate to macroscopic variables as $\langle\tau\rangle = \sigma_{\rm ext}/2$ and $\langle P_c\rangle = P_0 + \sigma_{\rm ext}/2$. The condition for sliding is given by a Coulomb local criterion, i.e., $\tau > \tau_{\rm st} = \mu P_c$. In the acoustic fluidization scenario first discussed by Melosh [8], in the presence of a vibration of frequency ω and local amplitude s, the normal stress becomes $P_c - s\sin\omega t$ and consequently the sliding condition reads $s_c = P_c - \tau/\mu$. Because of disorder, Melosh considers s as a stochastic variable with a Gaussian distribution of variance ς_s. Computing average displacement of grains per unit of time provides a way to estimate the effective viscosity of the medium. However, given that the only stochastic variable is s, viscosity diverges in the absence of sound which cannot account for our experimental observation of a finite viscosity. Therefore, we introduce a second stochastic variable p of null average and variance, ς_p, to account for the distribution of the local pressure. With this, the sliding condition is simply $y = s + p > y_c = \langle P_c\rangle - \tau/\mu$ and some contacts can slide even at external stresses below yield stress. Considering s and p as independent variables, the y variance is $\varsigma = \sqrt{\varsigma_s^2 + \varsigma_p^2}$, which leads to a generalization of Melosh's formula [9] for effective viscosity as

$$\eta \propto \left(2\mathrm{erfc}\left(\frac{1-\tau/\tau_{\rm st}}{\varsigma/y_c}\right)^{-1} - 1\right). \quad (5)$$

At this point, we hypothesize that $\varsigma_p = \beta\langle P_c\rangle$ and $\varsigma_s = \alpha\varsigma_p\epsilon_{\rm US}/d$, with α and β as proportionality constants. Notice that this hypothesis assures that in the absence of local variability of the internal pressure, i.e, completely homogeneous force network, the stochastic character of the acoustical pressure vanishes. With this, the effective viscosity change due to a sudden increase in the acoustic pressure is written

$$\frac{\Delta\eta}{\eta_+} = 1 - \frac{\mathrm{erfc}(\frac{y_c(\tau_{\rm st}-\tau)}{\tau_{\rm st}}\varsigma(\epsilon_{\rm US+})^{-1})}{\mathrm{erfc}(\frac{y_c(\tau_{\rm st}-\tau)}{\tau_{\rm st}}\varsigma(\epsilon_{\rm US-})^{-1})}, \quad (6)$$

with $\varsigma(\epsilon_{\rm US}) = \beta\langle P_c\rangle\sqrt{(\alpha\epsilon_{\rm US}/d)^2 + 1}$. In Fig. 4(b) our experimental data are fit to the previous formula by adjusting α and β for distinct values of $\sigma_{\rm ext}$. All curves can be fit by the same values of $\alpha = 5.8\times10^3$ and $\beta = 0.18$, which provides experimental support to our hypothesis regarding the distributions of both the internal pressure and the local sound amplitude.

In conclusion, this experimental study shows that relatively high intensity ultrasound induces softening and significant plasticity that can be both accounted for by introducing a fluidity and an effective aging parameter. The internal dynamic process giving rise to softening in the reversible regime is qualitatively consistent with the scenario described by Jia *et al.* in Ref. [4], where only the hysteresis in the force contact is at play. However, the tendency of softening to saturate with sound amplitude requires more investigation. Qualitatively, a crossover is observed above acoustic levels for which only tiny rearrangements (at the scale of asperities) take place; therefore, at high $\epsilon_{\rm US}$ the number of sliding contacts should dominate over the reversible ones. Finally, let us emphasize that an effective viscosity can be defined to account for the creep process. In the presence of ultrasound, a simple generalization of Melosh's model, along with a suitable choice of parameters characterizing internal stress distribution, account well for the experimental finding. However, at vanishing ultrasonic amplitude, the role of thermal activation or mechanical external noise is still an open and challenging issue and further effort would be required to develop microscopic models accounting for time evolution of the fluidity and the effective viscosity.

F. Melo is very grateful to Eric Clement for enlightening discussions. The support from contracts ANR-Fondecyt 011 and "Anillo" ACT95 is acknowledged.

[1] J. B. Knight, C. G. Fandrich, C. N. Lau, H. M. Jaeger, and S. R. Nagel, Phys. Rev. E **51**, 3957 (1995).
[2] J.-C. Géminard and H. Gayvallet, Phys. Rev. E **64**, 041301 (2001).
[3] V. B. Nguyen, T. Darnige, A. Bruand, and E. Clement, Phys. Rev. Lett. **107**, 138303 (2011).
[4] X. Jia, T. Brunet, and J. Laurent, Phys. Rev. E **84**, 020301 (2011).
[5] P. A. Johnson and X. Jia, Nature (London) **437**, 871 (2005).
[6] X. Jia, Phys. Rev. Lett. **93**, 154303 (2004).
[7] Y. Khidas and X. Jia, Phys. Rev. E **85**, 051302 (2012).
[8] H. J. Melosh, J. Geophys. Res. **84**, 7513 (1979) [http://www.agu.org/journals/jb/v084/iB13/JB084iB13p07513/].
[9] H. J. Melosh, Nature (London) **379**, 601 (1996).
[10] P. A. Johnson, H. Savage, M. Knuth, J. Gomberg, and C. Marone, Nature (London) **451**, 57 (2008).
[11] O. Zik, J. Stavans, and Y. Rabin, Europhys. Lett. **17**, 315 (1992).
[12] R. Snieder and J. Page, Phys. Today **60**, No. 5 49 (2007).
[13] C. Derec, A. Ajdari, and F. Lequeux, Eur. Phys. J. E **4**, 355 (2001).